



An assessment of independent component analysis for detection of military targets from hyperspectral images

K.C. Tiwari^{a,*}, M.K. Arora^a, D. Singh^b

^a Department of Civil Engineering, IIT Roorkee, Roorkee 247667, India

^b Department of Electronics and Computer Engineering, IIT Roorkee, Roorkee 247667, India

ARTICLE INFO

Article history:

Received 13 March 2010

Accepted 26 March 2011

Keywords:

Hyperspectral images

Spectral variability

Spectral matching algorithms

Anomaly detectors

Independent component analysis

ROC space

ABSTRACT

Hyperspectral data acquired over hundreds of narrow contiguous wavelength bands are extremely suitable for target detection due to their high spectral resolution. Though spectral response of every material is expected to be unique, but in practice, it exhibits variations, which is known as spectral variability. Most target detection algorithms depend on spectral modelling using *a priori* available target spectra. In practice, target spectra is, however, seldom available *a priori*. Independent component analysis (ICA) is a new evolving technique that aims at finding out components which are statistically independent or as independent as possible. The technique therefore has the potential of being used for target detection applications. A assessment of target detection from hyperspectral images using ICA and other algorithms based on spectral modelling may be of immense interest, since ICA does not require *a priori* target information. The aim of this paper is, thus, to assess the potential of ICA based algorithm *vis a vis* other prevailing algorithms for military target detection. Four spectral matching algorithms namely Orthogonal Subspace Projection (OSP), Constrained Energy Minimisation (CEM), Spectral Angle Mapper (SAM) and Spectral Correlation Mapper (SCM), and four anomaly detection algorithms namely OSP anomaly detector (OSPAD), Reed–Xiaoli anomaly detector (RXD), Uniform Target Detector (UTD) and a combination of Reed–Xiaoli anomaly detector and Uniform Target Detector (RXD–UTD) were considered. The experiments were conducted using a set of synthetic and AVIRIS hyperspectral images containing aircrafts as military targets. A comparison of true positive and false positive rates of target detections obtained from ICA and other algorithms plotted on a receiver operating curves (ROC) space indicates the superior performance of the ICA over other algorithms.

© 2011 Elsevier B.V. All rights reserved.

1. Introduction

Hyperspectral data, due to its high spectral resolution, appear to be the most attractive for various target detection applications particularly the military targets. The spectral response of an object in the natural world, however, does not exhibit a unique and deterministic signature, and may vary due to atmospheric interference, sensor noise, composition of the material, its location, surroundings, etc. This is known as spectral variability, which may also occur due to coarseness of the spatial resolution of the sensor. Full pixel target observations are, usually, corrupted by external noise, instrumental noise and atmospheric interference (Manolakis and Shaw, 2002).

Three families of mathematical models have been proposed in the literature to characterize the above spectral variability

(Manolakis et al., 2003). These models are: probability density models, subspace models and linear mixing models. In probability density models, the observed spectrum is modelled as multivariate normal distribution for the target and non-target classes both. In subspace models, the spectral variability is restricted to a limited number of bands instead of the complete band space. On the other hand, the linear mixing model assumes that the observed reflectance spectrum can be generated as a linear combination of a small number of deterministic spectral signatures of constituents known as the end members. Besides, a variety of other spectral variability models for extracting information from hyperspectral imaging have been proposed by several other researchers (Chang, 2001, 2003). These spectral models may facilitate development of several algorithms for extracting information such as target detection from hyperspectral data and can be grouped into two categories namely, spectral matching algorithms and anomaly detection algorithms (Manolakis, 2004).

Spectral matching algorithms are based on matching the known spectra of the targets of interest available from spectral libraries

* Corresponding author.

E-mail addresses: kcchtphd@gmail.com, kccht2000@yahoo.co.in (K.C. Tiwari), manojfec@iitr.ernet.in (M.K. Arora), dharmfec@iitr.ernet.in (D. Singh).

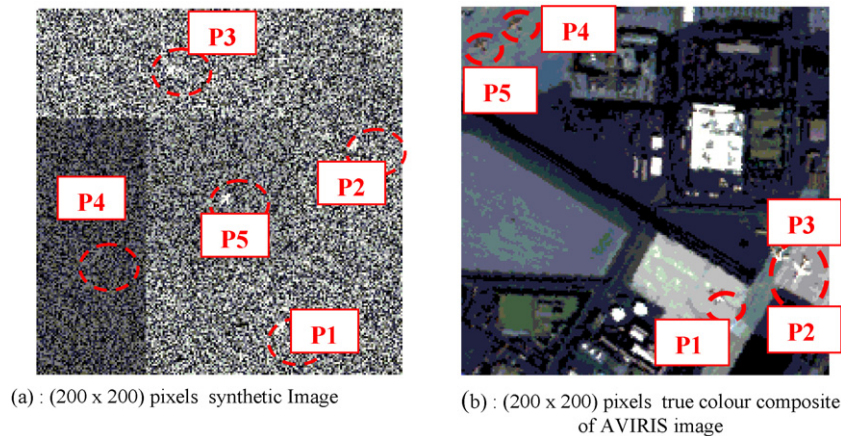


Fig. 1. Experimental data sets.

with the corresponding spectra from hyperspectral images. Spectral matching can be performed under the domain of any of the three spectral variability models. Anomaly detection algorithms do not require knowledge of spectra of targets of interest *a priori*. Anomaly detection is carried out with reference to a local background (*i.e.*, by considering only a part of the image) or global background (*i.e.*, by considering the whole image together). Every pixel, the spectral response of which does not fit a model of the local or global background, is treated as a candidate to be a target pixel.

Independent component analysis (ICA) is an evolving new technique for target detection. The goal of ICA is to find a linear representation of non-Gaussian data so that the components are statistically independent (Hyvarinen and Oja, 2000; Zhang and Zhu, 2009). The most common approach to seek statistical independence between random data is to minimize the mutual information between them. ICA results in statistically independent components and therefore the targets are likely to appear in one of the transformed independent components. In a target detection problem, most of the man-made targets in natural environment can be treated as statistically independent entities. Thus, ICA appears to be suitable technique for target detection from hyperspectral data (Zhang and Zhu, 2009; Stefan and Varshney, 2004). Further, the ICA does not require any *a priori* information about the targets and may still be able to segment independent sources, thus, detecting small and even hidden/camouflage targets. An alternative method of target detection in hyperspectral imagery combining ICA with local singularity too has been reported and found to perform superior to conventional RX algorithm (Wang et al., 2006).

The aim of this paper was to assess the performance of an ICA based algorithm (FastICA) for military target detection from hyperspectral images *vis a vis* some of the spectral matching and anomaly detection algorithms. The study shall be restricted to detection of fully resolved small targets only. The term 'small target' has been defined as follows, if the total number of pixels contributed by a single instance of a target in the image does not exceed 0.5% of the total pixels in the image ignoring the spatial resolution, it has been termed small target.

2. Experimental data

Two different hyperspectral datasets were selected keeping in mind the availability of reference information about the targets in these datasets. The first dataset was synthetically generated whereas the second dataset consists of an AVIRIS image.

2.1. Dataset I: synthetic image

To keep the experiments computationally simple, only 30 bands of synthetic images that matched the characteristics of the AVIRIS sensor were generated. Accordingly, the first 30 bands of the AVIRIS data set (band numbers 7 to 32 and 36 to 39) after removing bad bands and water absorption bands were selected as reference for generating the synthetic data. Further, to ensure spectral variability within the artificial military targets, and between these targets and the background, the following procedure was adopted.

First, each synthetic image was generated in five different segments each containing one target. The size of four of these segments was kept as 140×60 pixels whereas the size of the central segment was kept as 80×80 pixels. Next, the spectral reflectance values (intensities) of pixels in each segment were generated through a uniformly distributed random number generator applied within the same radiometric range as that of the AVIRIS image. A small target approximating the shape of an aircraft covering 18 pixels was inserted in each of these segments by replacing the existing intensities of these pixels in the synthetic image with reflectance values much higher than the mean reflectance values in that segment. The top left coordinates of five such targets consisting of 18 pixels are (30, 70), (70, 170), (170, 130), (130, 30) and (100, 100). The number of pixels of the target was restricted to 18 pixels only so that it constitutes less than 0.5% of the total number of pixels in the corresponding segment. A 200×200 pixels synthetic image, thus generated, corresponding to the first band of AVIRIS image and containing five small targets is shown in Fig. 1(a). These targets were given IDs as P1–P5.

2.2. Dataset II: AVIRIS image

An archived hyperspectral image (size: 400×400 pixels, 224 bands) from the AVIRIS sensor acquired over a naval air station in San Diego, California was used. The image is available as example data in the ENVI image processing software. After removing water absorption and bad bands, only 189 bands were considered for the analysis. Due to the effects of illumination from source and the atmosphere, the raw radiance spectra captured by any hyperspectral sensor need to be converted into reflectance spectra for effective comparison with laboratory spectra. The available image had already been converted to a reflectance image. Therefore, for the present case, a 200×200 pixels reflectance image containing five targets (aircrafts) were extracted for the study (Fig. 1(b)). The positions of these five targets (aircrafts) are centered at coordinates (244, 145), (232, 137), (199, 158), (89, 11) and (70, 22). These targets

have been given IDs P1–P5 as for the Synthetic images. It may be noticed that the last two targets (i.e., P4 and P5) fall under shadow.

In order to get the exact numbers of pixels that constitute each target of interest, five segments of size 12×12 pixels, each containing one aircraft were extracted from this 200×200 pixel image. Thereafter, Canny's edge detector filter was applied to each segment to detect edges of the target (aircraft). All pixels lying within these edges were considered as actual number of pixels constituting the target.

3. Methodology

The methodology includes several processing steps namely hyperspectral data representation and processing, implementation of ICA and other target detection algorithms and performance evaluation based on ROC.

3.1. Hyperspectral data representation and processing

In hyperspectral image analysis, information contained in any given pixel across several bands is considered as a vector of a K -dimensional space (K is equal to the number of spectral bands) (Stefan and Varshney, 2004). A hyperspectral image, therefore, consists of several pixel vectors, which in turn, can,

3.2. Independent component analysis

The goal of ICA is to find a linear representation of non-Gaussian data so that the components are statistically independent or as independent as possible (Hyvarinen and Oja, 2000; Zhang and Zhu, 2009). In the context of target detection, various bands of a hyperspectral image can be considered as K linear mixtures x_1, x_2, \dots, x_K composed of n independent components s_1, s_2, \dots, s_K . These components may consist of both the desired targets and redundant information in the form of undesired targets and noise. Mathematically, the j th mixture in this case can be represented as:

$$x_j = a_{j1}s_1 + a_{j2}s_2 + \dots + a_{jK}s_K \quad (1)$$

for all j

Rewriting Eq. (1) in matrix notation as:

$$x = As \quad (2)$$

Eq. (2) is also known as the ICA model. Denoting the columns of A as a_j , the ICA model can be rewritten as:

$$x = \sum_{i=1}^n a_i s_i \quad (3)$$

The ICA aims to find components which are statistically independent. A reference to Gaussian distribution will indicate that a necessary condition for the resulting components to be statistically independent is that these components will have non-Gaussian distribution. Further, in order to find independent components, a demixing matrix W is required. ICA provides possible solutions for estimation of the demixing matrix. This may be done by maximizing one of the measures of non-Gaussianity such as kurtosis (4th statistical moment) or negentropy (differential entropy). Alternatively, minimisation of the mutual information between the components can also be performed to find the demixing matrix W (Fig. 2).

FastICA algorithm, adopted in this study, is a negentropy based implementation of ICA and has been described in Hyvarinen and Oja (2000). Since all artificial targets in any natural background are expected to retain statistical independence, these are likely to get separated and appear in one of the ICA components.

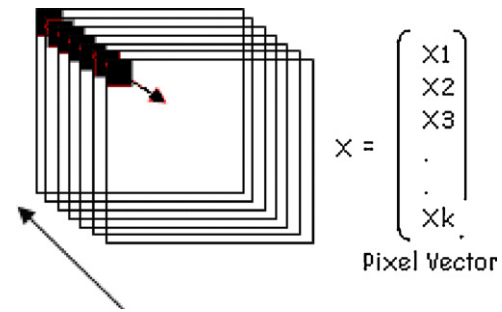


Fig. 2. Hyperspectral data representation using a pixel vector (note: each of the square window indicates different bands, x_1, x_2, \dots, x_K , etc., indicate pixel intensities in each band).

3.3. Other target detection algorithms

Two different categories of algorithms namely, spectral matching algorithms and spectral anomaly detection algorithms as discussed in subsequent paragraphs were used in this study.

3.3.1. Spectral matching detection algorithms

These algorithms attempt to identify pixels the spectrum of which exhibits a high degree of correlation (i.e., matching) to the known spectrum of the target of interest (reference spectrum) obtained either from spectral libraries or identified from the image in a supervised or unsupervised manner. Though, a large number of spectral matching algorithms have been reported in the literature, four algorithms namely, Orthogonal Subspace Projection (OSP) (Ren and Chang, 2003; Chang, 2005), Constrained Energy Minimisation (CEM) (Ren and Chang, 2003), Spectral Angle Mapper (SAM) (ERDAS) and Spectral Correlation Mapper (SCM) (ERDAS) were used in this study. The details of these algorithms can be found in the respective references given.

3.3.2. Spectral anomaly detection algorithms

These algorithms do not require knowledge of the reference spectrum of the targets of interest. If the spectrum of each pixel does not match with the spectrum of a local or global background, it is declared as an anomaly. The anomaly, however, may occur due to the existence of target or due to the atmospheric compensation or sensor error, etc. This seems to be the limitation of anomaly detection algorithms. The two commonly used anomaly detector algorithms are: orthogonal subspace anomaly detector (OSPAD) (Chang, 2005) and RX (named after Reed and Xiaoli, who proposed the algorithm) anomaly detector. There are two variants of the RX anomaly detectors namely UTD (uniform target detector) and RXD–UTD (a combination of both RX anomaly detector and the UTD) (Chang and Chang, 2002; O'Donnell, 2002). Details of all these algorithms can be found from the references given.

Thus, the following algorithms were considered in this study:

- (a) Independent Component Analysis (ICA)
- (b) Orthogonal Subspace Projection (OSP)
- (c) Constrained Energy Minimisation (CEM)
- (d) Spectral Angle Mapper (SAM)
- (e) Spectral Correlation Mapper (SCM)
- (f) Orthogonal Subspace Anomaly Detector (OSPAD)
- (g) Reed and Xiaoli Anomaly Detector (RXD)
- (h) Uniform Target Detector (UTD)
- (i) RXD–UTD (combination of Reed and Xiaoli Anomaly Detector and Uniform Target Detector)

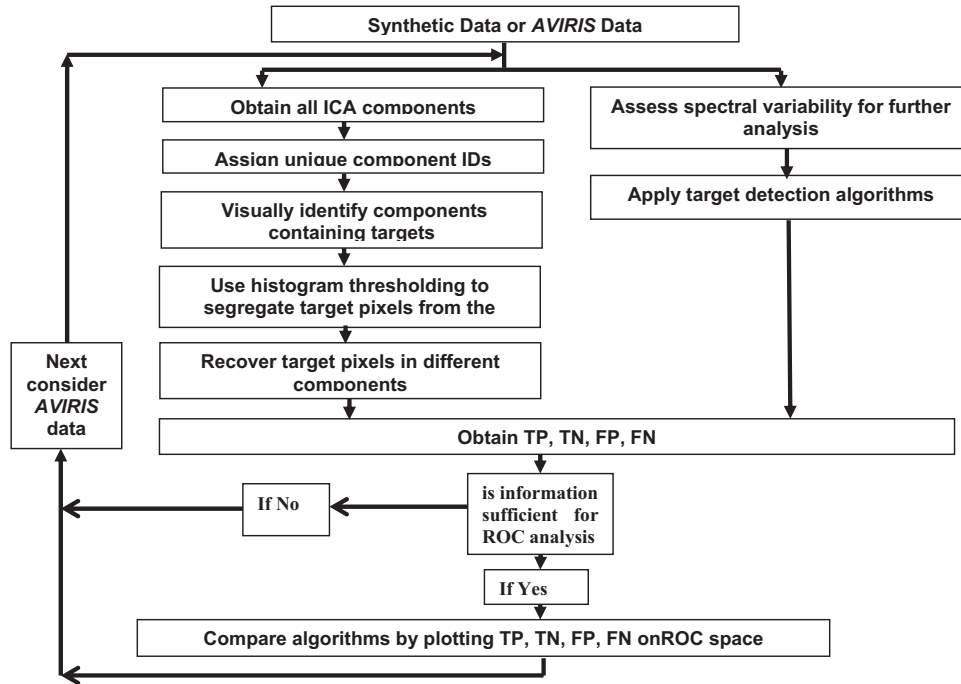


Fig. 3. Flowchart for implementation.

3.4. Performance evaluation of target detection algorithms

For a comparative assessment of the performance of the various target detection algorithms, an ROC curve analysis was considered which has been discussed here briefly.

The mathematical framework for detector design is a binary hypothesis testing problem, which can be solved using a variety of approaches. However, likelihood ratio (LR) test is usually preferred as it minimizes the risk associated with the incorrect decisions. Thus, for a given spectrum, x , the target detection problem can be cast as a selection between two competing hypotheses, namely, H_0 : target absent and H_1 target present. If $p(x|H_0)$ and $p(x|H_1)$ are the conditional probability density functions of x under the two hypotheses, the LR is given by:

$$LR(x) = \frac{p(x|\text{target present})}{p(x|\text{target absent})} \quad (4)$$

If $LR(x)$, also known as detection statistic, exceeds a certain threshold η , then the target present hypothesis is selected as true. Thus, the LR test accepts the most likely hypothesis as true. If the conditional probability densities in Eq. (4) are known, then this case is called a simple hypothesis and an optimal threshold can be selected easily. Naturally, the selection of threshold should be such as to keep the number detection errors (both target misses and false target detections) low and the number of correct target detections as high as possible. Therefore, a trade-off lies between a low threshold which keeps the number of correct detections (usually denoted by P_D) high, and a high threshold which keeps the false alarms, i.e., false target detections (usually denoted by P_{FA}) low. For any given detector, the trade off between P_D and P_{FA} can be described using the receiver operating (ROC) curves which plot $P_D(\eta)$ and $P_{FA}(\eta)$ as a function of all possible values of the threshold η . Therefore, ROC curves provide a means of evaluating the detector performance independent of the threshold. Various terms commonly associated with the ROC analysis and relevant to this study have been summarised as:

True positives (TP) = number of correct detections

True negatives (TN) = number of correct rejections

False positives (FP) = number of false detections/false alarm (also known as, Type I error)

False negatives (FN) = number missed detection (also known as, Type II error)

True positive rate (TPR) = i.e., hit rate = $TPR = TP/P = TP/(TP + FN)$

False positive rate (FPR) = i.e., false alarm rate = $FPR = FP/N = FP/(FP + TN)$

Often, values of the threshold η may not be explicitly known and in such cases, a comparison between the detectors can be carried out using an ROC plot obtained by plotting true positive rates along the y-axis and false positive rate along the x-axis and by determining the position of individual detectors on the ROC space. The lower left point (0, 0) represents a detection algorithm, which has neither any true positive rate nor any false positive rate, and is therefore of no use. Similarly, opposite of this, i.e., upper right point (1, 1) gives the same true positive and false positive and hence is irrelevant. The perfect detection therefore is the one represented by top left point (0, 1) which has zero false positive rate and the highest true positive rate. Similarly, the opposite of this, i.e., the point (1, 0) has the highest false positive rate and zero true positive rate and therefore indicates the worst performance.

3.5. Implementation of algorithms used

The sequence of implementation steps on both sets of data is given in Fig. 3 and elaborated below:

- (i) First, the experiments were carried out with synthetic data followed by AVIRIS data. In each case, all the ICA components were obtained and unique component IDs were assigned to them for further analysis. Next, all the ICA components containing any instance of the five targets (fully or partially) were visually identified and segregated. Since, no single ICA component

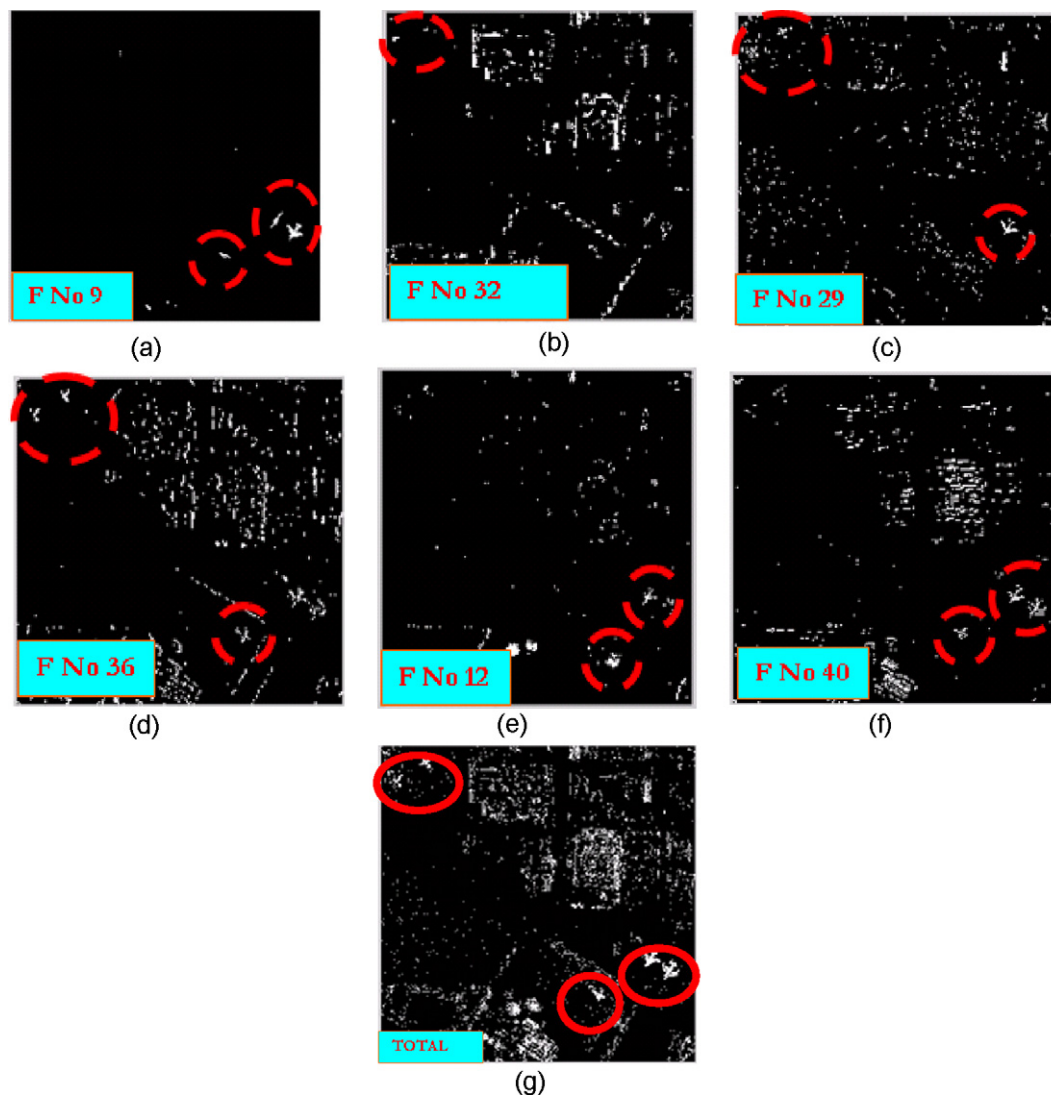


Fig. 4. Retrieving targets from various ICA components.

was likely to contain only the target pixels, hence, histogram thresholds were applied to each of these components to segment target pixels of various instances of the targets appearing in different components. Since it was possible that pixel vectors belonging to any one single instance of the target could appear in different components due to different illumination conditions or some other reasons, and since, no single ICA component was likely to contain all the pixel vectors of any given instance of a target, hence, in order to recover all the target pixel vectors belonging to any single instance of a target, the final image was obtained by adding up all the thresholded components.

- (ii) Simultaneously, target detection was carried out using various spectral matching and anomaly detection algorithms under study. However, since spectral variability is an important issue in the case spectral matching and spectral anomaly detection algorithms, an assessment of spectral variability present within various pixel vectors of each single instance of the target as well across different targets was carried out before implementing these algorithms. The spectral variability was assessed by randomly selecting five pixel vectors each from each of the five instances of the targets and plotting spectral measurements against the wavelengths (*i.e.*, bands). Next, for the purpose of target detection, one pixel vector for each

instance of the target was selected randomly and used as a reference spectrum for detection. While carrying out target detection, all the target pixel vectors detected, irrespective of whether they belonged to the same target from which the reference spectrum was drawn or not, were noted. This was done for each of the reference spectrum and both for spectral matching and anomaly detection algorithms.

- (iii) Next, in each case the true positives, true negatives, false positives and false negatives were determined using the reference data and it was analysed whether the information available was sufficient to be plotted on a ROC space.
- (iv) Finally, the performance of ICA was compared with various algorithms by plotting the results on a ROC space.

4. Results and discussions

The aim of the study being an assessment of performance of ICA vis a vis various other spectral matching and spectral anomaly detection algorithms, first, target detection using ICA are discussed followed by target detection using spectral matching algorithms and spectral anomaly algorithms. Further, though all the experiments were conducted first using synthetic data and then using AVIRIS data, the focus here is on AVIRIS data and hence wherever the results are same for both the synthetic data as well as AVIRIS

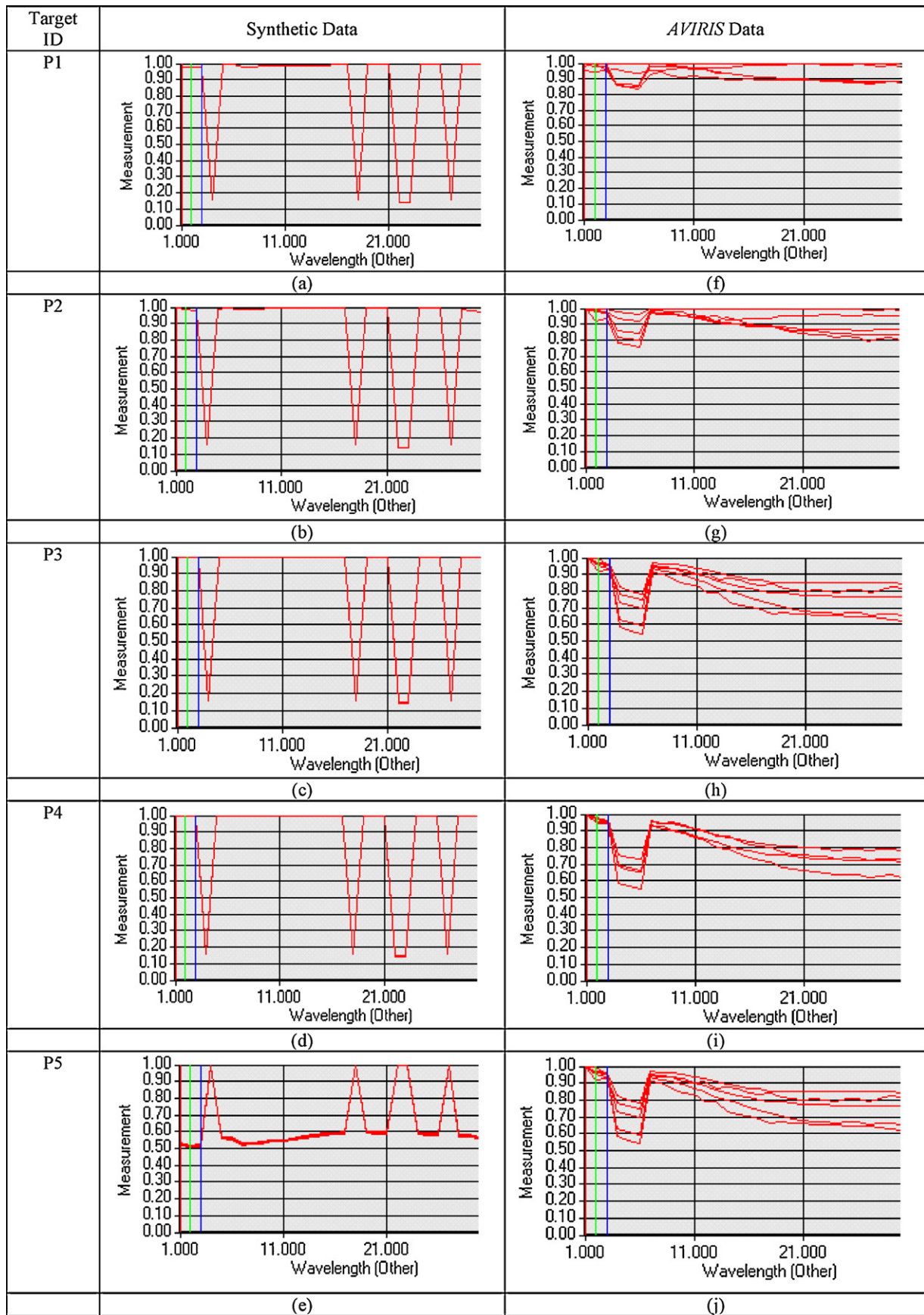


Fig. 5. Spectral variability exhibited by various targets synthetic data (a)–(e) and AVIRIS data (f)–(j).

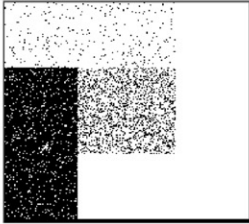
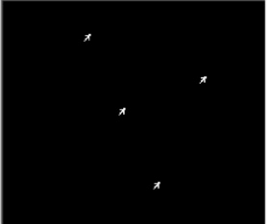
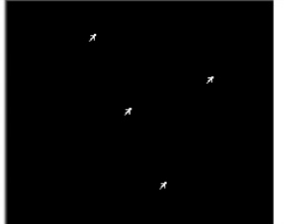
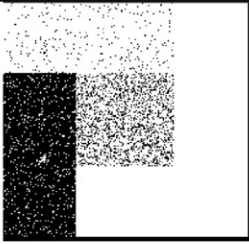
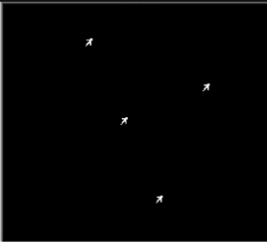
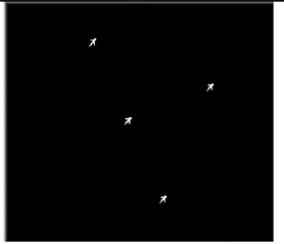
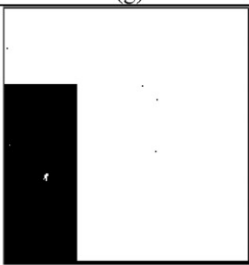
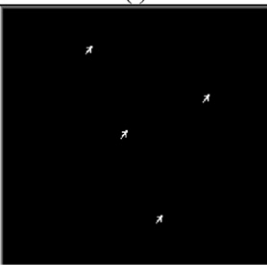
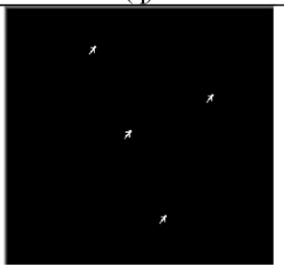
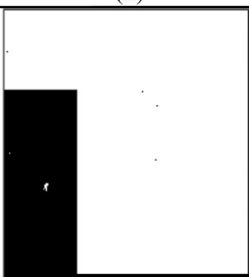
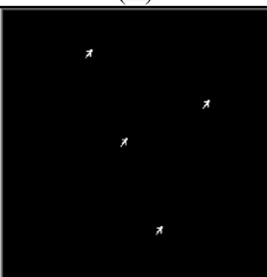
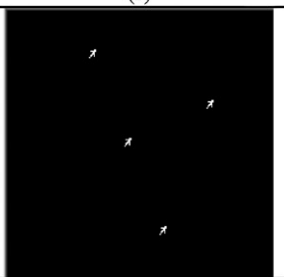
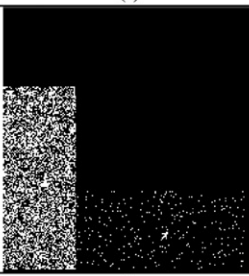
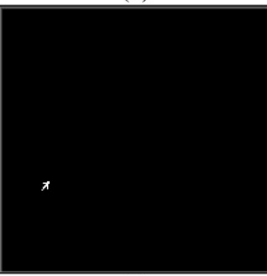
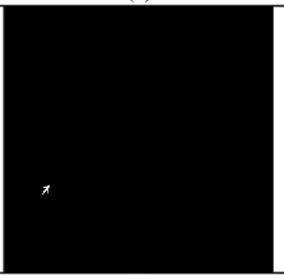
TD	OSP	CEM	SAM	SCM
P1	No Detection			
	(a)	(f)	(k)	(p)
P2	No Detection			
	(b)	(g)	(l)	(q)
P3	No Detection			
	(c)	(h)	(m)	(r)
P4	No Detection			
	(d)	(i)	(n)	(s)
P5	No Detection			
	(e)	(j)	(o)	(t)

Fig. 6. Target detection using spectral matching algorithms in synthetic data (TD, target detector).

data, results for only *AVIRIS* data are discussed. An ROC based comparative analysis is discussed at the end.

4.1. Target detection using ICA

ICA resulted in 30 components for synthetic data corresponding to each band of synthetic data. For *AVIRIS* data, however, only 187 components out of 189 bands were retained rejecting the last two components due to the large number of iterations involved in

data processing. Each of these components were assigned a unique component ID for further analysis.

Next, the components containing targets were found by visual inspection for both the datasets. For the synthetic data, four ICA components were found to contain the targets but no single component was found to contain all five targets. Each of these components, however, also contained certain redundant information. It was, therefore, necessary to extract those pixels, which constituted the target. This was done through segmentation. A histogram of the

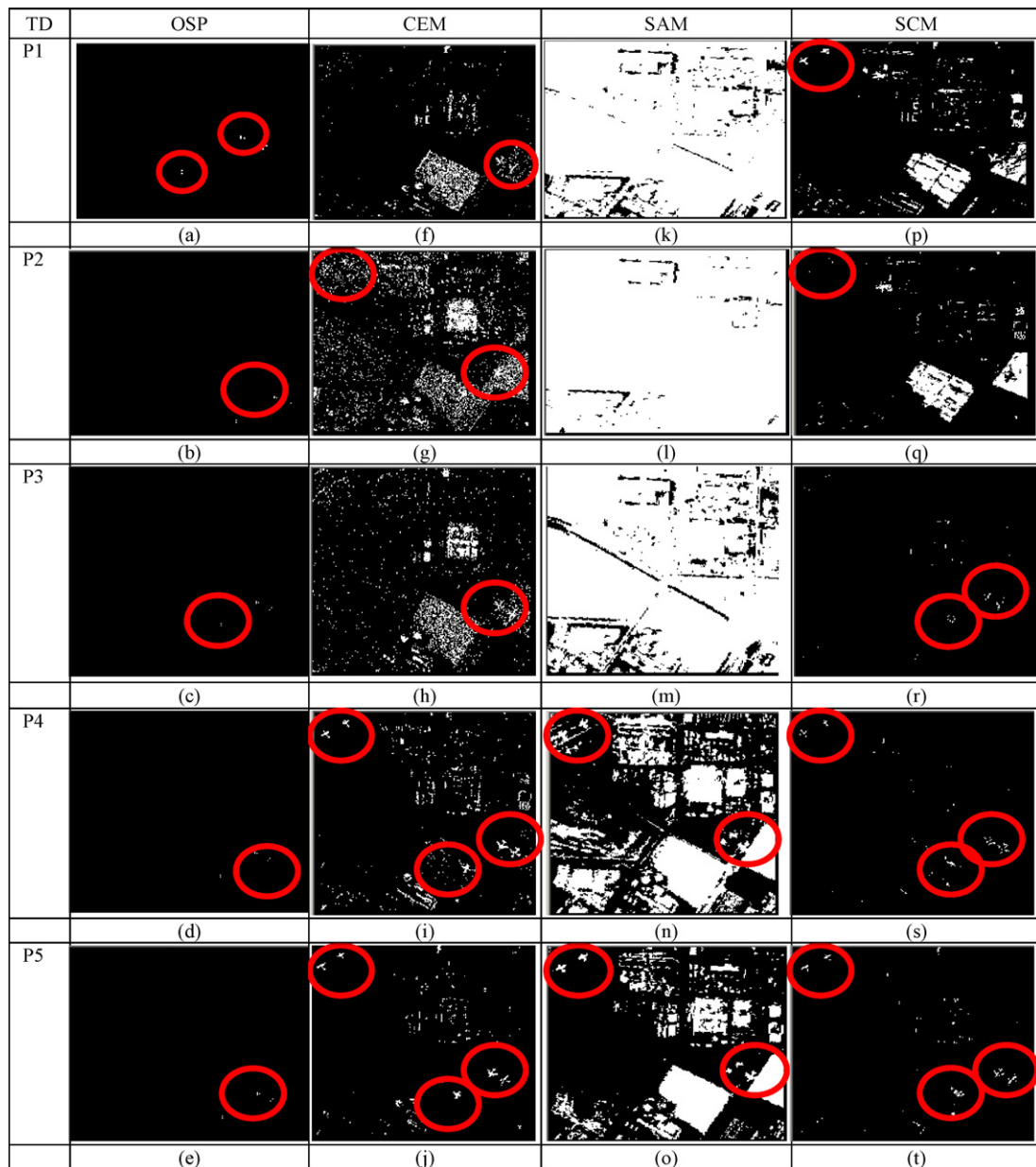


Fig. 7. Target detection using spectral matching algorithms in AVIRIS data (TD, target detector).

image was generated and a threshold value was selected to segment the target from the rest of the image. This process led to the creation of a binary image.

4.2. Target detection using spectral matching and spectral anomaly algorithms

Spectral variability being the most important issue in target detection in hyperspectral images, it was necessary to assess the spectral variability present in the data. For assessment of spectral variability, five different pixel vectors (*i.e.*, five different spectrum) per target (P1–P5) were considered and plotted as shown in Fig. 5. Line plots were generated with wavelength along the *x*-axis and corresponding intensities (scaled on 0–1) along the *y*-axis. Each individual plot indicates spectral variability within a single instance of a target both in synthetic images (Fig. 5(a)–(e)) and AVIRIS images (Fig. 5(f)–(j)).

A similar procedure was adopted for the AVIRIS data. In this case, however, there were fifteen components that contained the targets but no single component was found to contain all the five targets. Further, it was found that all the components were not necessary to recover all the pixels of the targets. Therefore, the first six components out of the 15 components were selected, which together contained pixels of all five targets. Components containing targets were segmented using histogram based thresholding to generate six binary images (Fig. 4(a)–(f)). These binary images were then integrated to recover all the targets (Fig. 4(g)). The integrated binary image formed the basis for subsequent ROC analysis for the assessment of the ICA algorithm. The procedure being same for both the Synthetic and the AVIRIS data, only the results for AVIRIS data have been shown here.

On analysis of the line plots for the synthetic data, it may be noticed that all the five spectra corresponding to five different pixels completely overlap each other indicating that no single instance of the synthetic target exhibits any spectral variability

within itself. Similarly when the spectra of different synthetic targets (P1–P5) are considered, limited or no spectral variability is noticed (Fig. 5(a)–(e)). On the other hand, spectral variability is evident both within each single instance of the AVIRIS target as well as across its different instances (Fig. 5(f)–(j)).

After examining spectral variability, one spectrum (pixel vector) per target P1–P5 of synthetic data was drawn randomly and, thus, five different reference spectra, one each corresponding to targets P1–P5 were considered. The results of target detection achieved on implementation of the four spectral matching algorithms on synthetic data using each of the five reference spectrums (corresponding to targets P1–P5) are shown in Fig. 6. The four spectral matching algorithms implemented are shown on the top row of the figure while the left column shows the ID of the target from which the reference spectrum was drawn to implement the algorithm. The results were produced as binary images with 1 (white pixel) showing a match with the reference spectrum and 0 (black pixel) showing a mismatch. Once the detections were made using various spectral matching algorithms, detected pixels per image were compared with the true target pixels already noted as described in Section 2 to arrive at the deductions made here. OSP fails in all the cases as shown in Fig. 6(a)–(e) and CEM produces lots of false alarms as shown in Fig. 6(f)–(j). Both SAM (Fig. 6(k)–(n)) and SCM, Fig. 6(p)–(s) appears to perform much better than OSP and CEM. However, it can also be noticed that both SAM and SCM have been able to detect targets P1–P4 using reference spectrum from any of the targets P1–P4. But the fifth target P5 is detected using only its own spectra (Fig. 6(o) and (t)). The reason for this may be attributed to greater spectral variability exhibited by the spectra of P5 as shown in Fig. 5(e).

A similar procedure was adopted for AVIRIS data. Here again, one spectrum (pixel vector) per target P1–P5 of AVIRIS data was drawn randomly and, thus, five different reference spectra, one each corresponding to target P1–P5 were considered. The results of target detection achieved on implementation of the four spectral matching algorithms on AVIRIS data using each of the five reference spectra (corresponding to targets P1–P5) are shown in Fig. 7. The four spectral matching algorithms implemented have been shown on the top row of the figure while the left column shows the ID of the target from which the reference spectrum was drawn to implement the algorithm. The results were produced as binary images with 1 (white pixel) showing a match with the reference spectrum and 0 (black pixel) showing a mismatch. Once the detections were made using various spectral matching algorithms, detected pixels

per image were compared with the true target pixels already noted as described in Section 2 to arrive at TP, FP, TN and FN (refer ROC analysis discussed in Section 3 and later in this section). These values are given in Table 2. Certain deductions have been made as discussed here after analysis of the values obtained for TP, FP, TN and FN and on visual examination of the results.

Fig. 7(a)–(e) shows pixels containing target detected using OSP. From the results, it can be noticed that OSP appears to be very sensitive to spectral variability and leads to detection of only a few pixels containing targets. Further, on comparing these figures with Fig. 1, it can be noticed that irrespective of the reference spectrum, the detected target pixels belong to any of the three targets P1, P2 or P3. OSP has not been able to detect any of the target pixels belonging to targets P4 and P5 which are under the shadow. The other algorithm which appears to be sensitive to spectral variability is CEM. The results are shown in Fig. 7(f)–(j). In this case, reference spectrum of even a single instance of the target (e.g., P4) succeeds in detecting most of the targets. But it also raises several false alarms in each case. The results from SCM are shown in Fig. 7(p)–(t), which indicate that the algorithm is successful in detecting all the targets including P4 and P5, though any single reference spectrum (P1–P5) does not detect all the targets. However, SAM, which is known to be insensitive to illumination, produces lot of false alarms as shown in Fig. 7(k)–(o). Next the two anomaly detection algorithms were also applied as shown in Fig. 8. In case of AVIRIS data, the result of OSP anomaly detection was found to be almost similar to the OSP spectral matching algorithm as shown in Fig. 7(a). None of the other three anomaly detection algorithms, i.e., RXD, RXD–UTD and UTD yields any detection for AVIRIS data. In case of synthetic data, it was found that OSP anomaly detector does not yield any detection, however, the other three anomaly detection algorithms, i.e., RXD, RXD–UTD and UTD are able to detect all the targets in the synthetic data as shown in Fig. 8(f)–(h). The reason for anomaly detectors not being successful with the AVIRIS data but being successful with synthetic data appears to be the fact that the synthetic data has limited spectral variability. Due to lack of sensitivity of anomaly detectors towards the spectral variability, anomaly detection algorithms were not been considered further for comparative assessment with ICA.

4.3. Comparative assessment using ROC

Finally, a comparative assessment of ICA with various spectral matching algorithms was performed. Synthetic targets, which

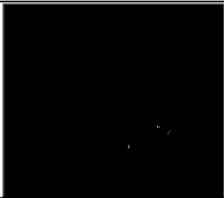
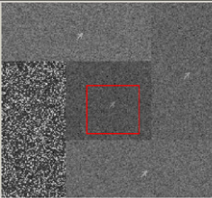
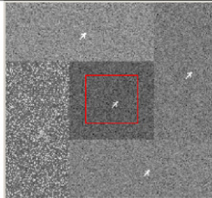
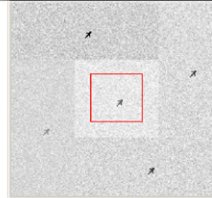
Anomaly Detectors	OSPAD	RXD	RXD-UTD	UTD
Detections in AVIRIS Data		No Detection	No Detection	No Detection
	(a)	(b)	(c)	(d)
Detections in Synthetic Data	No Detection			
	(e)	(f)	(g)	(h)

Fig. 8. Target detection using anomaly detection algorithms.

gives too little true positive detections. In target detection applications, detection of a few true positive pixels as made by OSP may not substantiate a target. Similarly, CEM produces high true positive rates but also produces equally high false positive rates. The performances of SCM and SAM have also not been found to be satisfactory as both these algorithms produced high false positives rates.

5. Conclusions

The aim of this paper was to assess the applicability of an ICA based algorithm for military target detection and its comparative assessment with four spectral matching algorithms, namely OSP, CEM, SAM and SCM, and four anomaly detection algorithms, namely OSP anomaly detector, RXD, RXD-UTD and UTD. A set of synthetic and *AVIRIS* images were used for the study.

The spectral variability analysis showed that targets in a synthetic image had limited or nil spectral variability while the *AVIRIS* targets exhibited significant spectral variability both within each target as well as across different targets.

This was further corroborated through the difference in performance of various spectral matching and anomaly detection algorithms. From the results on target detection from *AVIRIS* dataset, it appears that OSP is very sensitive to spectral variability and therefore while the number of true positive pixels detected is low, the numbers of false positive pixels are also extremely low. Therefore, the high sensitivity of OSP may be useful in applications where only presence is to be substantiated such as detection of presence of gases. Both CEM and SCM were also found to be sensitive to spectral variability but the numbers of false positive pixels in the case of CEM was the highest. The performance of SAM was, however, found to be the poorest.

The experiments were conducted in a similar manner for the synthetic data which exhibits little spectral variability. Here, OSP fails completely and CEM produces a lot of false positives. In this case, both SAM and SCM produce the most appropriate results with high true positive pixels and almost nil false positive pixels.

In case of anomaly detectors for *AVIRIS* data, the OSPAD produced results similar to OSP but RXD, RXD-UTD and UTD failed to detect any target. On the other hand, for synthetic data, however, OSP anomaly detector failed completely. All the other anomaly detectors although successful in detecting the targets also produced high false positive pixels.

In summary, in case of targets which are likely to show spectral variability, OSP, SCM and CEM are likely to perform better. Anomaly detectors are likely to fail in such cases. On the other hand, in case of limited or no spectral variability, SAM and SCM are likely to perform better and may be preferred. Anomaly detectors are also likely to be successful though with high false positives.

Finally, to assess the ICA algorithm with other spectral matching algorithms, ROC curves were generated. From the location of ICA on the ROC plot, it is evident that the performance of ICA is superior to other spectral matching algorithms. Further, ICA has an additional advantage in the sense that it does not require any *a priori* information.

References

- Chang, S.S., 2001. Unsupervised target detection in hyperspectral images using projection pursuits. *IEEE Transactions on Geosciences and Remote Sensing* 39 (7), 1380–1391.
- Chang, C.I., 2003. *Hyperspectral Imaging—Techniques for Spectral Detection and Classification*. Plenum Publishers, New York, USA.
- Chang, C.I., 2005. Orthogonal subspace projection (OSP) revisited: a comprehensive study and analysis. *IEEE Transactions on Geoscience and Remote Sensing* 43 (3), 502–518.
- Chang, C.I., Chang, S.S., 2002. Anomaly detection and classification for hyperspectral imagery. *IEEE Transactions on Geoscience and Remote Sensing* 40 (6), 1314–1325.
- ERDAS Imagine Spectral Analysis Users Guide, ERDAS Imagine V 8.6.
- Hyvarinen, A., Oja, E., 2000. Independent Component Analysis: Algorithms and Applications. Neural Networks Research Centre, Helsinki University of Technology, Neural Networks, <http://www.cs.helsinki.fi/u/ahyvarin/papers/NN00new.pdf>.
- Manolakis, D., 2004. Detection Algorithms for Hyperspectral Imaging Applications: A Signal Processing Perspective. MIT Lincoln Laboratory, 0-7803-8350-8/04/\$20.00 © 2004/IEEE.
- Manolakis, D., Shaw, G.A., 2002. Detector algorithm for hyper spectral imaging application. *IEEE Signal Processing Magazine* 19 (1), 23–43.
- Manolakis, D., Marden, D., Shaw, G.A., 2003. Hyperspectral image processing for automatic target detection applications. *Lincoln Laboratory Journal* 14 (1), 79–115.
- O'Donnell, E., 2002. Final Report on Implementation of the Rx Algorithm. ENVI, Inc., USA.
- Ren, D.Q., Chang, C.I., 2003. A comparative assessment for orthogonal subspace projection and constrained energy minimisation. *IEEE Transactions on Geoscience and Remote Sensing* 41 (6), 1525–1529.
- Stefan, A.R., Varshney, P.K., 2004. Further Results in Use of Independent Components Analysis for Target Detection in Hyperspectral Images., <http://www.cs.uno.edu/stefan/>.
- Wang, C., Zhang, J., Gu, Y., 2006. Target detection for hyperspectral images using ICA-based feature extraction. In: *IEEE International Conference on Geoscience and Remote Sensing Symposium, IGARSS 2006*, pp. 850–853.
- Zhang, J., Zhu, F., 2009. Target detection approach for hyperspectral imagery based on independent component analysis and local singularity. In: *Fifth International Conference on Natural Computation*, vol. 2, pp. 603–607.